Conductive Polymer Composites Synthesized from Diacetylene-Functionalized Linseed Oil and MWCNT: Gamma Irradiation and Organic Vapor Sensing

A. Ramírez-Jiménez[1]*, S. Hernández López[1], E. Bucio[2] and E. Vigueras Santiago[1]

[1]*Laboratory of Research and Development of Advanced Materials, Faculty of Chemistry, UAEMex, Toluca, CP 50120, Mexico*
[2]*Department of Radiation Chemistry and Radiochemistry, Nuclear Sciences Institute, National Autonomous University of Mexico, Circuito Exterior, Ciudad Universitaria, Mexico DF 04510, Mexico*

ABSTRACT: Epoxidized linseed oil (ELO) was synthesized and functionalized with propargylamine (PA) or 3-ethynylaniline (EA) and the products were crosslinked to obtain the diacetylene-functionalized epoxidized linseed oil polymers which were used as matrices in the preparation of the composites with multiwalled carbon nanotubes (MWCNTs). Electrical resistance at percentages between 4 and 20 wt/wt% of filler was measured and the percolation threshold was calculated, obtaining 1.2 and 1.7% for the composites with EA and PA respectively. Low critical concentration evidenced a good dispersion of the MWCNTs without necessity of any modification. The final products were used in the sensing of acetone, chloroform and ethanol. The electrical resistance changes were measured at different concentrations and the sensibility was calculated. In order to improve stability toward the vapors, composites were irradiated with gamma rays and new sensing was done and compared. The results showed differences in sensibility, selectivity and reproducibility.

KEYWORDS: Gamma radiation, MWCNT, plant oils, polymer composites, vapor sensing

1 INTRODUCTION

Plant oils represent a good alternative to the need to produce materials and chemicals from renewable sources and therefore have been of great interest both in academia research and for industrial applications [1, 2]. Of these, soybean and linseed oils are attractive due to their low price, abundance and the high content of double bonds in their fatty acids [3–5]. This last feature makes them easy to modify by chemical conversion to other functional groups; among these modifications, epoxidation is one of the most used [6] because after epoxidation these groups may react by themselves by catalytic reaction or with other groups as acids, amines, alcohols, phenols or thiols in order to have specific functional groups into their structure [7–11]. Also, through the use of multifunctional reagents, the oxyrane rings can be used as crosslinker sites to obtain polymers; of these, amines are the most used due to their nucleophilic character. This versatility is

the reason why epoxy polymers have also been used in diverse applications ever since their commercial production in the middle of the last century [12]. In this work, we used linseed oil, which is a triglyceride consisting of three fatty acids condensed into a glycerol unit, with a composition mainly of linolenic acid (56.6%), linoleic acid (15.3%), and oleic acid (19.1%) moieties (Figure 1); on average it has 6.4 double bonds in its structure [5, 13].

On the other hand, carbon nanotubes (CNTs) have excellent electrical and mechanical properties [14, 15] which make them candidates for several applications, for example, as nanofiller material in conductive polymeric compounds [16], due to the large aspect ratio of CNTs being more effective compared with carbon black microparticles. The incorporation of CNTs into polymeric compounds gives rise to new opportunities for electronic applications, for example, in conductive films [17, 18], photovoltaic devices [19] or sensors [20–22]. Their advantages are that they may be flexible, easy to mold and cheap. Nonetheless the polymeric matrices have the same drawbacks as polymers from fossil sources. In these composites it is very important that there be a good and homogeneous dispersion of the

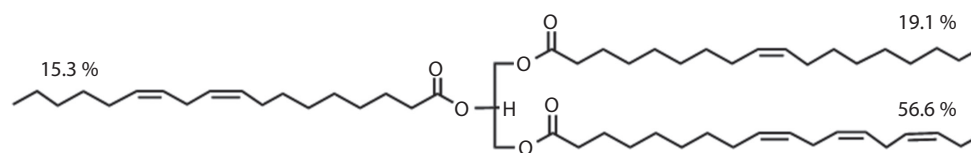*Corresponding author*: alejandro.ramirezj@tectijuana.edu.mx

Figure 1 Chemical structure and main composition of linseed oil.

conductive particles throughout the polymer matrix in order to obtain an effective and reproducible utilization; however, this main drawback is likely owing to van der Waals forces between them along their structure, where they form clusters or tight long bundles which might form a dense entangled network. Therefore, to improve the dispersion, surface modifications have to be done [23, 24]. One of these modifications is the noncovalent attachment of molecules, although its disadvantage is that the forces between the molecules and the CNTs might be weak. Another modification is the covalent attachment of functional groups to the CNT walls; however, this decreases their conductivity owing to the fact that the groups might introduce defects on the graphitic structure [25, 26]. Functionalization with divalent adducts is a better option since there is less alteration of the electrical transport because the sp^2 conjugation is retained [27]. Other options have been dispersion by shear mixing using surfactants [28] or by sonication in an adequate solvent [29, 30]. In order to avoid any modification to the CNTs and loss of the electrical properties, we have synthesized matrices with functional groups rich in electrical density without polar moment, such as diacetylenes, that can interact via van der Waals forces with the electrical density of the CNTs, assisting with their dispersion.

With respect to sensing, there is currently a need for flexible, mechanically robust and environmentally stable chemical vapor sensors with high efficiency and low power consumption. In this context, polymer/carbon black (CB) or CNT composites have been investigated for the detecting of organic solvent vapors [31, 32]; characteristics of these polymer composites are their easy preparation, low cost and sensing at room temperature. The detection mechanism is well explained by the percolation theory; this means that the electrical resistance is a function of the conductive filler concentration. During the sensing experiment, the composite suffers swelling, which produces disconnection of the electric paths. Once the solvent is evaporated, the paths are formed again, although they likely do not return to their initial conformation. For example, Hernández-López and coworkers [31] studied the sensing of tetrahydrofuran (THF) using a cellulose/CB composite. For each sample they registered

an initial electrical resistance (Ro), after which they introduced small volumes of THF. After introducing these small volumes they observed that the Ro did not return to its original value. They explained that this effect could be the result of solvent retention or a structural modification in the conductive network. These results are the main drawback of these sensors due to the fact that the reproducibility could become low.

On the other hand, is well known that ionizing radiation induces crosslinking and scission in polymers [33]; the first effect predominates if the chain is formed mainly of C-H bonds. So in order to override the drawback mentioned above, in this work the composites were irradiated with gamma rays at different doses to induce crosslinking and the effect in the sensing was evaluated.

2 EXPERIMENTAL SECTION

2.1 Materials

Lipase acrylic resin from *Candida antartica*, MWCNT DXL 110–170 nm × 5–9 mm (ρ = 1.9 g cm^{-3}), linseed oil (LO), hydrogen peroxide, alumina, anhydrous zinc chloride, PA, EA, copper chloride and tetramethylethylenediamine (TMEDA) were obtained from Sigma-Aldrich Co.; sodium carbonate and magnesium sulfate anhydrous were obtained from J.T. Baker, Mexico. All the reactants were used as received. SEM images were obtained using a JEOL JSM-6510LV microscope at acceleration voltage of 25 kV, at 10000X, with a back-scattered electron detector. The ^{1}H NMR spectra were recorded at room temperature using CDCl$_3$ as solvent on a Bruker Avance 300 MHz NMR. Chemical shifts are relative to $(CH_3)_4$Si and are given in ppm. The FTIR-ATR spectra were recorded on a Shimadzu FTIR-ATR Prestige 21 spectrophotometer, in a range between 550 and 4000 cm^{-1}; spectra were acquired at 4 cm^{-1} resolution and signals averaged over 32 scans. DSC and TGA analyses were recorded under nitrogen atmosphere (100 ml/min) using a SDT-Q600 TA Instruments modulus, from 20 to 600 °C and heating rate of 20 °C min^{-1}. Glass transition temperatures were determined using a DSC TA Q200 TA Instruments modulus; DSC measurements were recorded in modulation mode under nitrogen flow of 50 ml min^{-1} from −60 to 100 °C, heating rate

of 5 °C min⁻¹ with an amplitude of ±1 °C over a modulation period of 60 s; for DAPAELO, 5 mg were placed into aluminum hermetic pans and for DAEAELO, 2 mg were placed into the pans. For sensing, the initial electrical resistance was measured with a digital multimeter. Thickness of the samples was measured by a profilometer by Sloan Dektak IIA.

2.2 Synthesis of ELO

The ELO was synthesized using the chemoenzymatic method described in a previous report [34]: a toluene solution, 100 g (0.114 mol) of LO, 8 g (0.028 mol) of oleic acid and 10 g of lipase were put into a precipitate glass using 120 mL of solvent. The reaction mixture was warmed between 40–42 °C and mixed by stirring at 355 rpm, and then 160 mL of hydrogen peroxide at 30% was added drop by drop. After 24 hours, the reaction was filtered to recover the enzyme. The product was purified by successive extractions of 3 × 20 mL of Na_2CO_3 solution at 10% and 1 × 20 mL of water. Finally, ELO was dried using $MgSO_4$ anhydrous. The product was characterized by FTIR-ATR, ^1H NMR, DSC and TGA.

2.3 Synthesis of ELO Functionalized with Alkynes

For synthesis of functionalized ELO with the alkynes, a mixture of 0.5 g (0.5 mmol) of ELO, $ZnCl_2$ 0.014 g

(0.1 mmol) and 0.5 mL of PA (7.8 mmol) or 0.5 mL of EA (4.8 mmol) was heated at 80 °C for 5 h; the reaction was followed by FTIR-ATR. Color changes were observed from white to amber and red. Remainder alkynes were extracted with water and the products were filtered and solved in acetone; finally, they were dried by a rotary evaporator and by a vacuum line. The products, PAELO and EAELO, were characterized by FTIR-ATR, ^1H NMR, DSC and TGA.

2.4 Coupling of Terminal Alkynes

In order to obtain the polymer, C-C coupling of terminal acetylenes was carried out at room temperature by the Hay reaction (Figure 2) [35, 36]. PAELO or EAELO were dissolved in chloroform while an aqueous solution of CuCl and TMEDA in stoichiometric ratio 1:1 was prepared; both solutions were placed together and mixed by magnetic stirring under an air flow. After a few seconds a film on the surface was observed, which was removed, and then a new film was formed and removed again. This process was repeated until the film was not observed. The Cu(TMEDA) catalyst obtained *in situ* [37] was extracted with water as many times as necessary until the characteristic blue color was not observed. The final products were a yellow solid for diacetylene PAELO (DAPAELO) and a brown solid for diacetylene EAELO (DAEAELO), which were dried and characterized by FTIR-ATR, DSC and TGA.
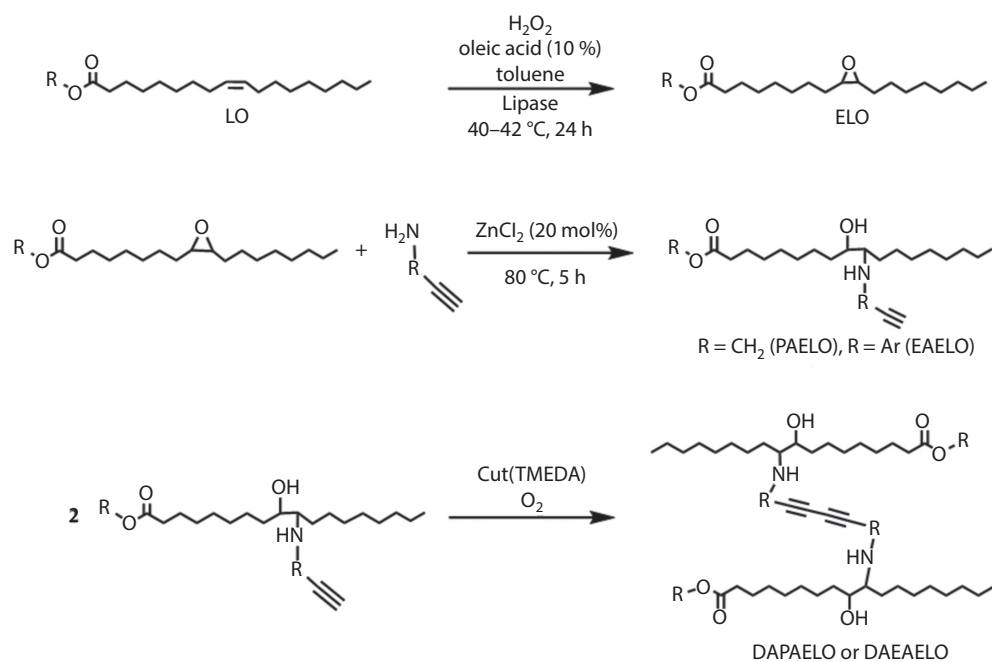

Figure 2 Simplified scheme for the synthesis of the polymeric matrices.

2.5   Preparation of the Polymeric Composites

The diacetylene-polymer composites (DAELO/MWCNT) were prepared in three steps. First the polymers between 8 and 9.6 mg/mL and MWCNT at concentrations between 0.4 and 2 mg/mL were dispersed in chloroform by an ultrasonic bath for 30 min at 35 MHz and 70 W. In the second step, equal volumes of dispersions were mixed and placed in the ultrasonic bath for 30 min more. Finally, 1 mL of these final solutions were placed inside stainless steel cylinders of 14 mm diameter mounted on glass plates. The solvent was evaporated slowly (casting technique) and the films were placed in an oven at 60 °C. Once the samples were dried, silver contacts were placed as parallel lines at 1 cm. In order to compare the effect of diacetylenes in the polymeric structure, ELO-polymer composites were made under the same conditions; owing to the fact that ELO is a liquid monomer, the films of the mixture on glass substrates were cured at 220 °C for 2 h in a vacuum stove, obtaining a solid composite due to the epoxy ring opening [38] and reaction between them.

2.6   Percolation Threshold

The electrical resistance of the films was measured, their resistivity was calculated and plotted against MWCNT percentage (wt/wt), and four samples were averaged for each point. The electrical resistance was measured at potentials between 10 and 100 mV; in all cases a lineal relation was observed. The percolation theory was applied in order to calculate the percolation threshold at the onset of the network; electrical resistivity obeys the power law relation:

$$\sigma = \sigma_m (\phi - \phi_c)^\beta$$

where σ is the electrical resistivity of the polymeric compound, ϕ is the filler concentration, ϕ_c is the critical filler concentration or percolation threshold and β and σ_m are fitting constants. The adjustment was made using Origin 6.0 software. Three free parameters, σ_m, ϕ_c and β, were considered [39], where σ_m is the proportionality constant. A data correlation of 0.99 was reached for running numerical interactions. The best fitting curves were obtained for β very close to -2.8 and -2.1, then β was fixed to this value and numerical interactions were run again.

2.7   Vapor Sensing

Sensing experiments were carried out for the electrical resistance changes to ethanol, acetone and chloroform vapors in which increasing volumes of 0.1, 0.2, 0.3, 0.4 and 0.5 mL of the solvents were injected into a sensing chamber with a dry and oil-free air flux of 5 L min^{-1}, as previously described [31, 32]. The maximum resistance was measured and plotted at real time for each set of pulses; between each pulse the samples were left in the air flux until they reached a minimal constant value. Sensibility was calculated using the equation:

$$S\ (\%) = 100\ \%\ [(R_m - R_0)/R_0]$$

where R_m and R_0 are the maximum and initial electrical resistance measured respectively.

2.8   Irradiation and Vapor Sensing

Samples with 6% (wt/wt) of MWCNT were chosen to be irradiated. The samples were exposed to ^{60}Co γ-ray source (Gammabeam 651 PT, MDS Nordion) at room temperature in a vacuum sealed borosilicate glass tube at rate doses between 8 and 11 kGy h^{-1}, and total doses of 10, 20, 30, 40 and 50 kGy. Volumes of 0.2, 0.3 and 0.4 mL of acetone or chloroform were injected. Their sensibility was calculated and compared with the value before irradiation.

3   RESULTS AND DISCUSSION

3.1   Synthesis

The ELO synthesized using the chemoenzymatic method obtained a very high double bond conversion. ELO was characterized by ^{1}H NMR, FTIR-ATR and DSC. The ^{1}H NMR spectrum showed the signals from epoxy ring between 2.90 and 3.21 ppm, which integrated for 11.5 hydrogens or 5.75 epoxy groups on average (Figure 3b). These signals allowed us to calculate the epoxy percent, which was 97%, with respect to the signals from the double bonds between 5.23 and 5.42 ppm in the ^{1}H NMR spectrum of LO, which integrated for 11.8 hydrogens, meaning 5.9 double bonds (Figure 3a); whereas in the ELO spectrum, the hydrogens from double bonds integrated only for 0.56. Molecular weight of LO and ELO was calculated by integration of their respective spectra. For the first one, its molecular weight was 879 g mol^{-1} and for ELO it was 977 g mol^{-1} using this data, and the epoxide number was 5.89 equiv kg^{-1} or 9.42 weight percent of oxirane, which is similar to that previously reported using this method [40]. In the FTIR spectrum the band at 821 cm^{-1} corresponding to the ν(**C-O**) from epoxy group was observed (Figure 4b) and those corresponding to the double bonds at 1650 and 3008 were not (Figure 3a). In DSC an exothermic process between 201 and 275 °C (Figure 5) was observed which corresponds to the ring opening of epoxy groups [41], and another exothermic process was observed between
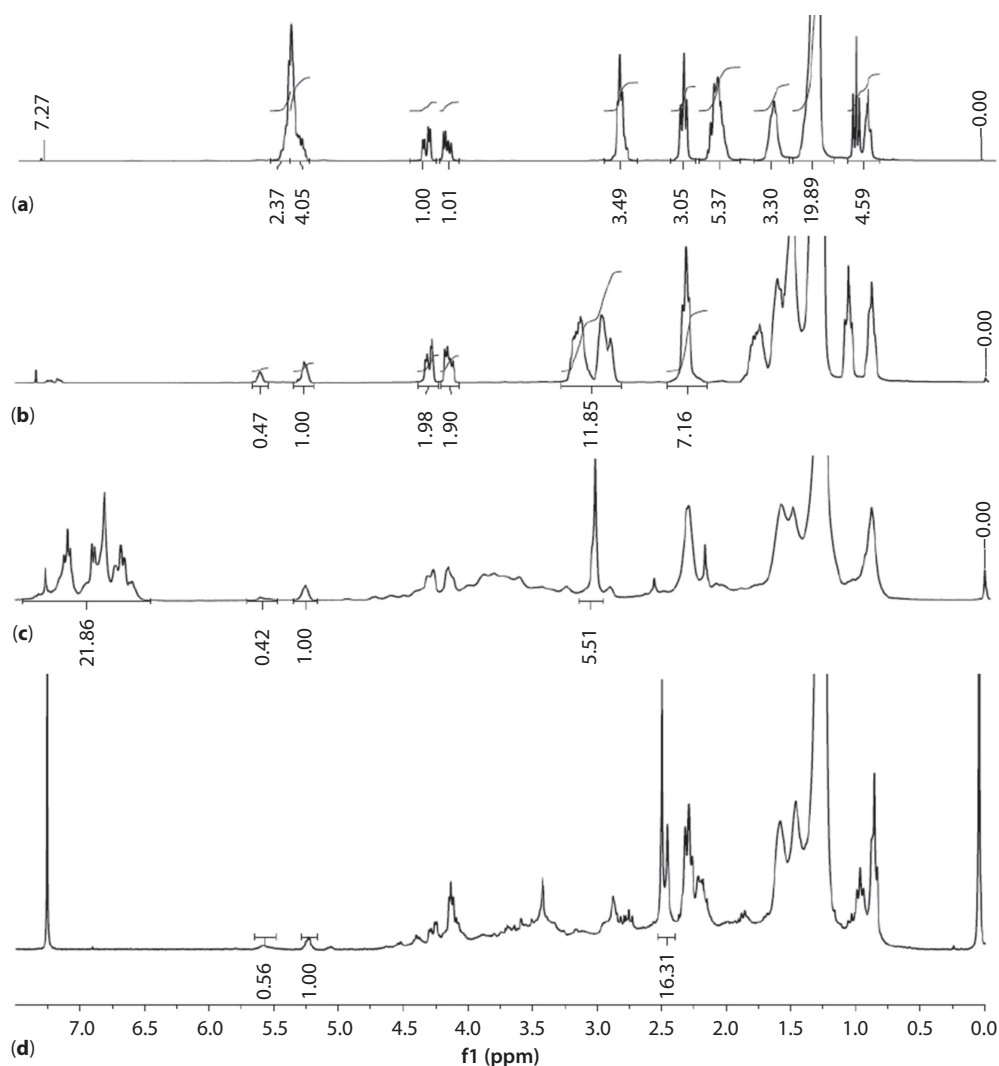
Figure 3 ^{1}H NMR 300 MHz, CDCl$_3$ spectra of (**a**) LO, (**b**) ELO, (**c**) EAELO and (**d**) PAELO.

155 and 200 °C, which could be due to the break of some ester groups [42].

The ELO was functionalized with PA or EA by an epoxy ring opening reaction catalyzed by ZnCl$_2$. The products were characterized by FTIR-ATR and ^{1}H NMR. In the FTIR-ATR spectra the bands of v(C≡**C-H**) at 3282 cm^{-1} and v(**C≡C**) at 2104 cm^{-1} for terminal alkynes and the characteristic one centered around 3450 cm^{-1} from hydroxyl groups were observed (Figures 4 and 6). In the spectrum of EAELO, one broad band at 3387 cm^{-1} corresponding to the secondary amine was observed; however, in the spectrum of PAELO this was not evident (Figure 6c). On the other hand, in the ^{1}H NMR spectrum of EAELO a singlet at 3.01 ppm is observed which corresponds to the terminal alkyne, the integration of the signals from the aromatic ring between 6.6 and 7.1 ppm, 21.84 hydrogens, allowed calculating 5.46 aromatic groups,

which indicated 95 percent of functionalization with respect to the 5.75 epoxy groups (Figure 3c). Whereas in the ^{1}H NMR spectrum of PAELO, the signals at 2.48 and 2.52 ppm corresponding to the terminal alkyne and the methylene group, respectively, integrated for 13.2 hydrogens, which allowed calculating 4.4 propargyl groups or 77% of functionalization (Figure 3d). These results contrast with expectations because of the higher nucleophilic character of the aliphatic amine with respect to the aromatic one [12]. However, the result for PAELO is only an approximation due to the fact that the secondary amine formed could react with another epoxy group due to its similar reactivity with respect to the primary one.

The C-C coupling was carried out by the Hay reaction. Polymerization was evidenced by the film formation on the solvent surface; it was removed and a kind of fiber was observed. In the FTIR-ATR spectrum
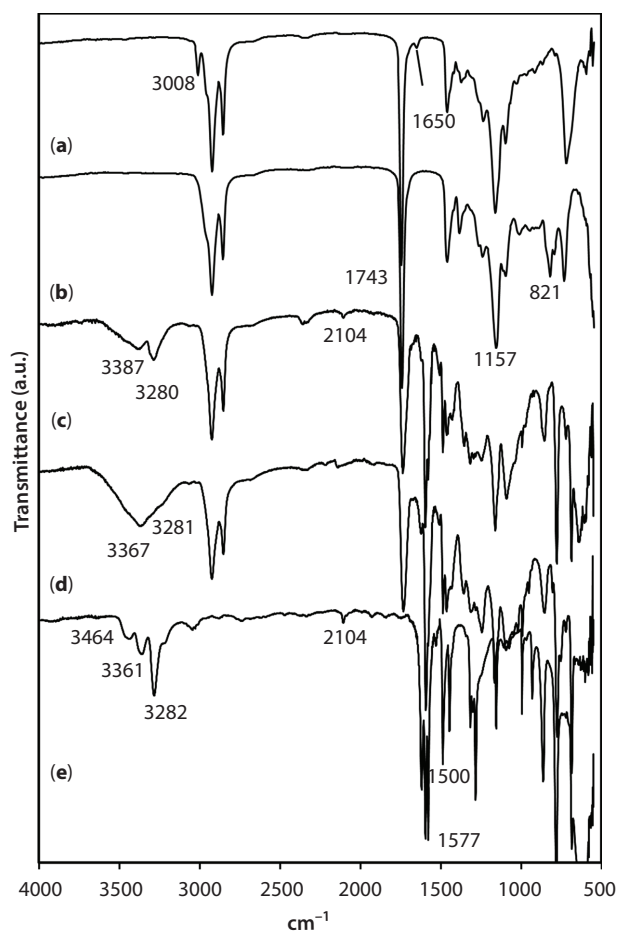
136   *J. Renew. Mater.*, Vol. 5, No. 2, April 2017

© 2017 Scrivener Publishing LLC

Figure 4 FTIR-ATR spectra of (**a**) LO, (**b**) ELO, (**c**) EAELO, (**d**) DAEAELO and (**e**) EA.

Figure 5 FTIR-ATR spectra of (**a**) LO, (**b**) ELO, (**c**) PAELO, (**d**) DAPAELO and (**e**) PA.

of DAEAELO the intensity of the band at 3282 cm^{-1}, corresponding to terminal alkyne, is lower than in the EAELO spectrum (Figure 4d). The same was observed in the spectrum of DAPAELO. This also allowed us to confirm the C-C coupling. Thermal stability was evaluated by TGA; in the thermograms of EAELO a weight loss of around 7% is observed between 100 and 180 °C. This could be owing to the loss of volatiles and low molecular weight components as water in the samples due to the presence of hydrophilic hydroxyl groups in the chains, residual EA and solvent. The 10% weight loss of EAELO at 271 °C was lower than DAEAELO and ELO at 328 and 365 °C respectively (Figure 7). For DAPAELO, the 10% weight loss was at 285 °C. These results indicated that the coupling gave a slight thermal stability with respect to functionalized ELO. The glass transition temperature was evaluated by DSC; for the polymeric network with PA its T_g was observed around −10 °C, whereas for the polymer with EA this was around 25 °C (Figure 8). These results were interesting because they help to

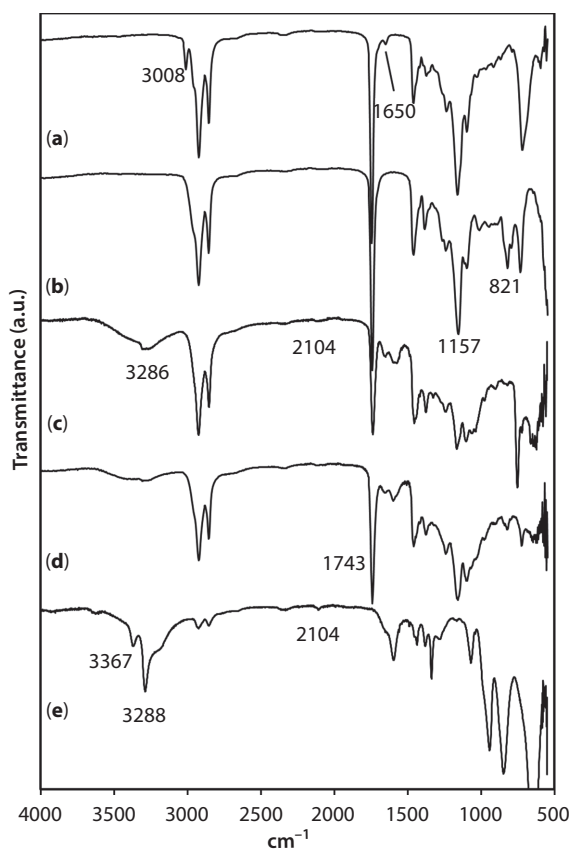better understand the differences in their behavior in the sensing test due to DAPAELO being less hard than DAEAELO at room temperature.

The composites were made as previously mentioned in the experimental section; chloroform was chosen as solvent because it has been used at high MWCNT concentrations [43]. A result of interest is that only 1 hour was enough to disperse MWCNT, inasmuch as longer times might cause fractures on CNT [44]. MWCNTs were mixed with the respective DAELO at 4, 6, 8, 10, 12, 16 and 20 (wt/wt), dispersion was confirmed by their conductivity and SEM images where samples with 10% of MWCNT at 10 000X were observed (Figure 9). DAEAELO composite polymer attached to CNT was observed owing to a major interaction with the aromatic rings. Once the dry films were obtained and contacts were placed with silver paint, the electrical resistance was measured and the resistivity was calculated; to calculate it, the area and the thickness of the films were measured. Note that the resistivity for DAPAELO and DAEAELO composites is lower than ELO composites with the same load of MWCNT (Table 1). The average values of four samples
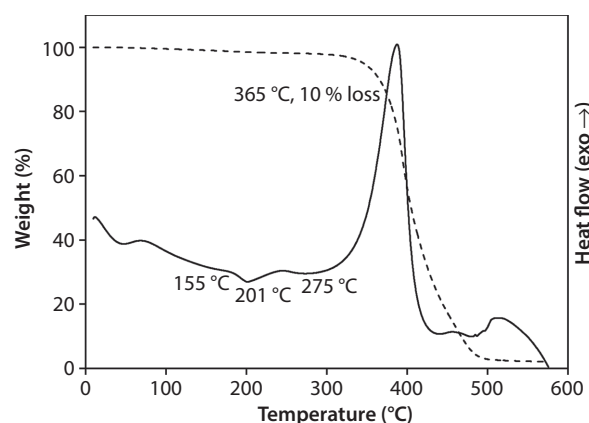
Figure 6 TGA (dashed line) and DSC (solid line) of ELO; heating rate of 20 °C min^{-1} under nitrogen atmosphere.
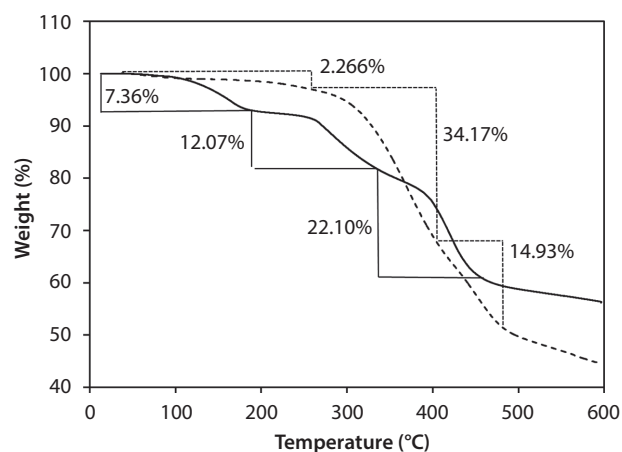
Figure 7 TGA of EAELO (solid line) and DAEAELO (dashed line); heating rate of 20 °C min^{-1} under nitrogen atmosphere.
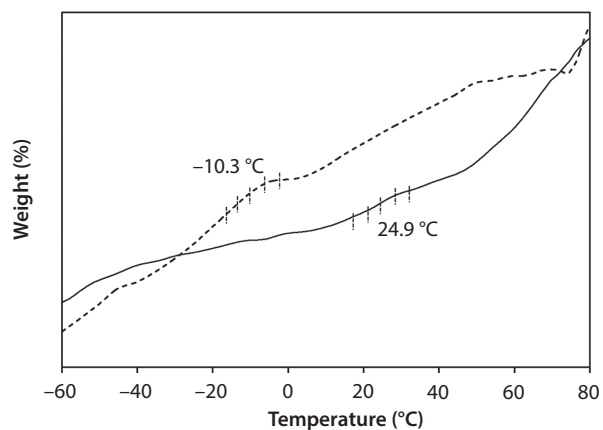
Figure 8 DSC in modulation mode of DAEAELO (solid line) and DAPAELO (dashed line) with amplitude of ± 1 °C over a period of 60 s; heating rate of 5 °C min^{-1}.
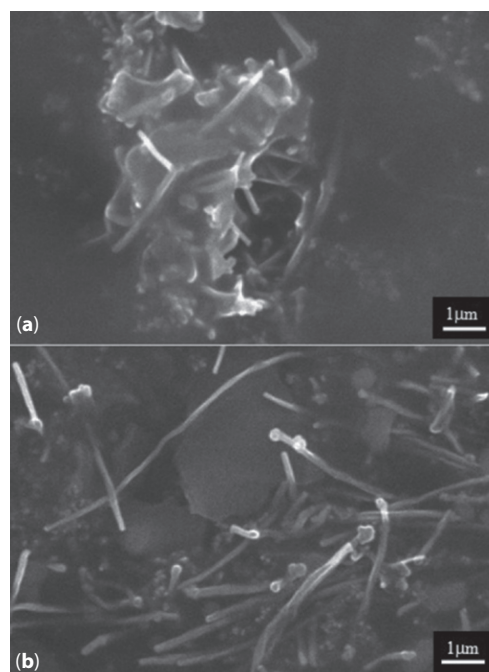

Figure 9 SEM micrographs of polymeric composites: (**a**) DAEAELO/MWCNT 10% and (**b**) DAPAELO/MWCNT 10%, 25 kV and 10 000X.
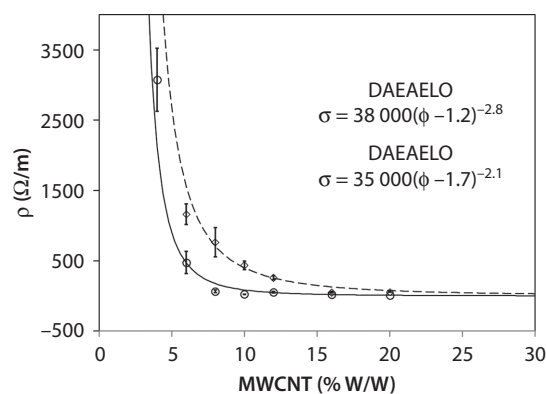

Figure 10 Resistivity as a function of MWCNT percentage of DAEAELO (solid line) and DAPAELO (dashed line) composites and their adjusted curves. Mean value ± SD (n = 4).

for each point were adjusted by the percolation threshold equation, finding the critical concentration (f_c) to be at 1.2 and 1.7% for DAEAELO and DAPAELO respectively. Data were plotted against MWCNT percentage (Figure 10). These values are similar to other polymer-MWCNT composites. For example, the percolation threshold for polystyrene/single-walled carbon nanotube composites was at 1.5% [45], for polyvinylidene fluoride/MWCNT it was at 0.95% [46] and for

Table 1 Calculated resistivity of composites at different loads of MWCNT. Mean value ± SD (n = 4).

MWCNT (wt %)	ρ (kΩ m^{-1}) DAPAELO/MWCNT	ρ (kΩ m^{-1}) DAEAELO/MWCNT	ρ (kΩ m^{-1}) ELO/MWCNT
4	–	3074.8 ± 449.8	
6	1161.9 ± 46.5	475.9 ± 158.6	4697 ± 1642
8	763.4 ± 207.6	65.25 ± 19.21	5711 ± 3658
10	434.3 ± 61.4	24.27 ± 3.30	3160 ± 944
12	258.4 ± 25.3	52.13 ± 12.37	3101 ± 1392
16	47.94 ± 3.67	20.61 ± 1.38	4697 ± 1642
20	54.74 ± 4.17	8.98 ± 0.74	
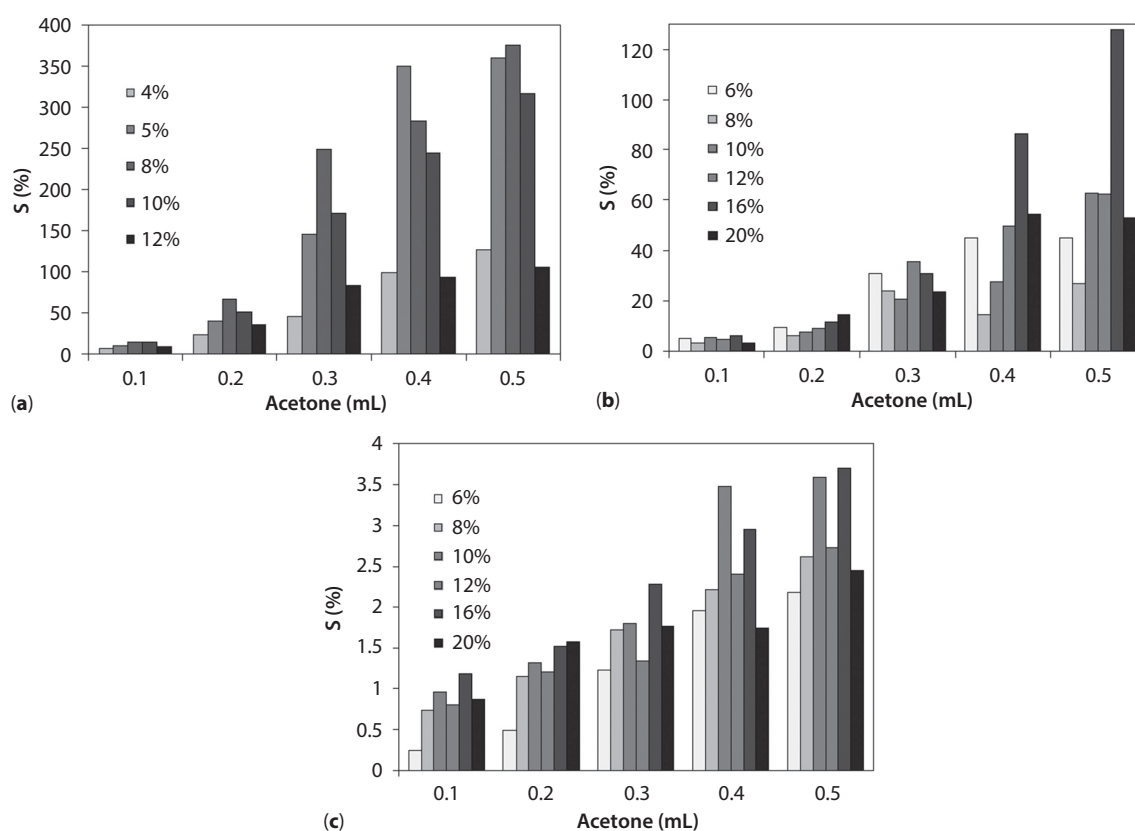
Figure 11 Acetone sensing using composites at different filler loads: (**a**) DAPOHELO, (**b**) DAPAELO and (**c**) DAEAELO.

DAELO/MWCNT crosslinked with propargyl alcohol, reported in our previous work, it was at 0.96% [47].

3.2 Sensing

Acetone sensing behavior of the composites at different filler concentrations in a progress experiment is shown in Figure 11. In these experiments, composites prepared previously with propargyl alcohol were included (DAPOHELO) [47]. In all cases it was

observed that the higher the volume of the pulse, the higher the sensibility. For ethanol and chloroform the same behavior was observed.

Composites with 6% of MWCNT were chosen to compare the sensing of chloroform, acetone, and ethanol. The results shown in Figure 12 confirm that DAPOHELO and DAPAELO had high sensibility toward chloroform. This behavior could be due to the polarity, since chloroform is the less polar solvent of these, which indicates that there is a high interaction
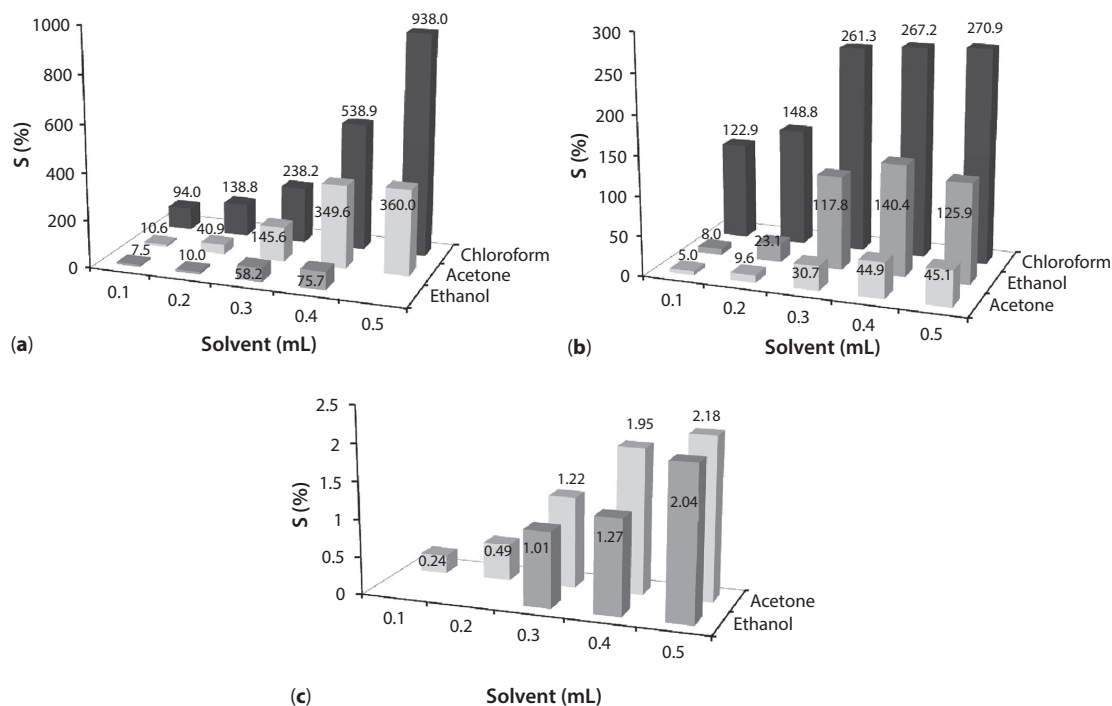
Figure 12 Comparative sensing of solvents using (**a**) DAPOHELO, (**b**) DAPAELO and (**c**) DAEAELO with 6% of MWCNT.

between the solvent and the hydrocarbon chains in the matrix. For acetone and ethanol, the sensibility for DAPOHELO had the behavior expected according to the polarity, which means it was more sensitive to acetone than ethanol. Whereas with DAPAELO an opposite effect was observed, meaning that other interactions affect the sensing, which in this case may be the hydrogen bond formation. On the other hand, in the sensing with DAEAELO composites, detectable changes were not observed for chloroform; for acetone and ethanol sensibility values were very low, which could be due to a high interaction between the matrix and the MWCNT as is observed in the SEM image (Figure 9), also because its Tg was relatively high, around 25 °C, which indicated that this material is hard at the temperature at which the sensing was done and therefore the swelling is not fast enough. The matrix had a high electronic density with the introduction of diacetylenes which also had aromatic rings, so this interaction does not allow swelling of the polymeric matrix by the solvents.

Samples of 1×1.2 cm of DAPOHELO and DAPAELO with 6% of MWCNT were chosen to evaluate the electrical resistance changes in the sensing of acetone and chloroform. The sensing was carried out before and after irradiation of the samples with gamma rays at doses of 10, 20, 30, 40 and 50 kGy. Intermediate pulses of 0.2, 0.3 and 0.4 mL were injected into the sensing

camera; each pulse was repeated four times in order to carry out the corresponding statistical analysis.

The results showed a diminishing sensibility toward acetone (Figure 13); however, the standard deviation in the irradiated samples was lower than in the non-irradiated ones, which indicated a better reproducibility; this effect could be observed at doses higher than 20 kGy. This result could be explained because radiation induced crosslinking in the polymeric matrices, thereby the swelling sample may return to the initial conformation. On the other hand, in chloroform sensing an opposite effect was observed (Figure 14) owing to the high affinity of the matrices toward this solvent; in this case a faster diffusion due to a diminishing thickness could be the cause of a higher sensibility. The thickness diminished from 7.4 to 5.8 mm in DAPOHELO and from 7.7 to 7.2 mm in DAPAELO composites at an irradiation dose of 20 kGy.

4 CONCLUSIONS

The synthesis of two polymeric matrices was carried out in three easy steps: (1) obtaining ELO functionalized with PA or EA by a catalytic ring opening reaction in order to have terminal acetylene groups; (2) coupling of C-C to form terminal acetylene groups which serve as crosslinkers to obtain the polymers; and (3) the mix
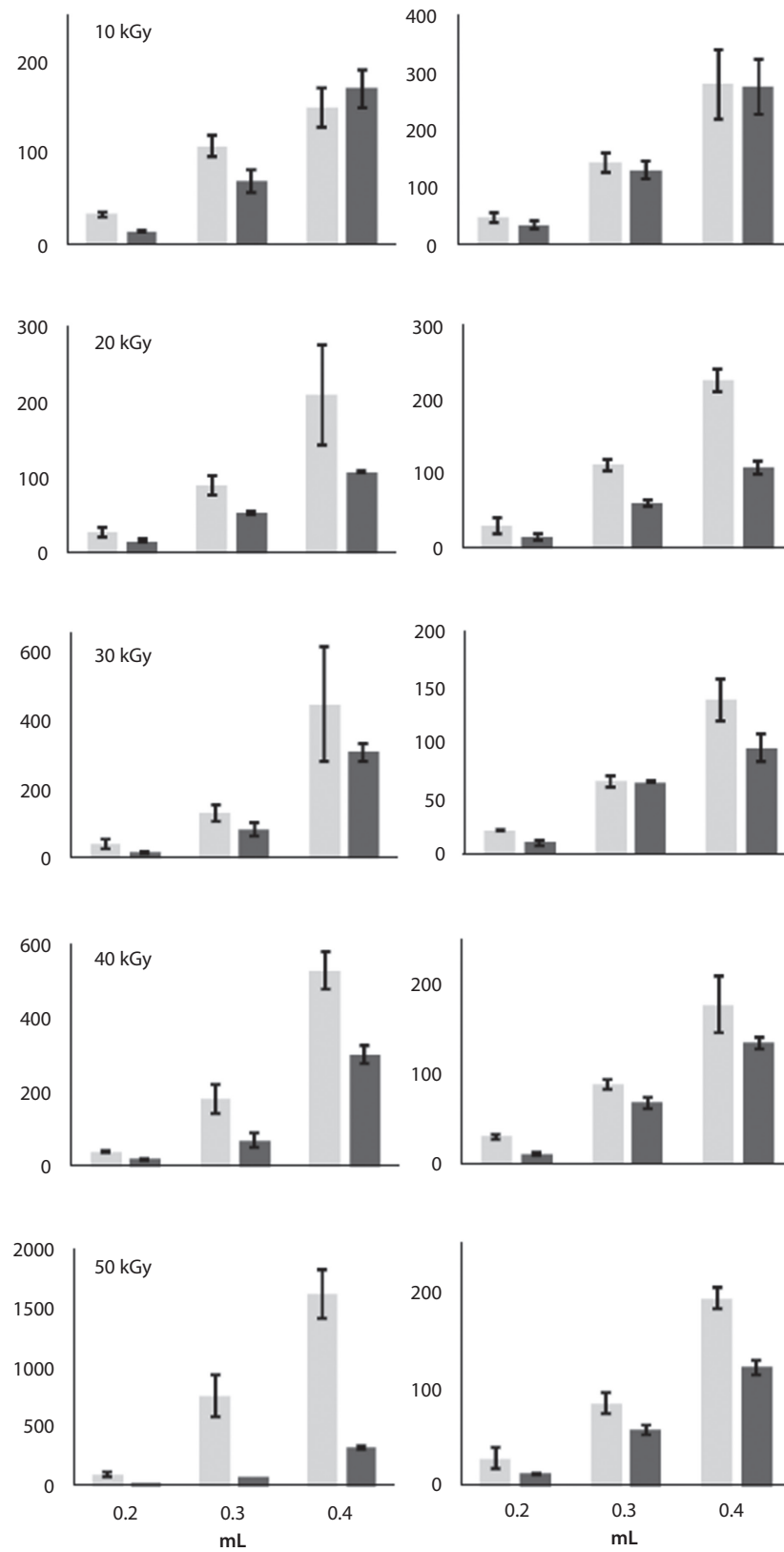
Figure 13 Comparative of sensibility (%) at different injection volumes of acetone. DAPOHELO/MWCNT (left) and DAPAELO/MWCNT (right). Light grey (no irradiated samples), dark grey (irradiated samples at different doses). Mean values ± SD (n = 4).
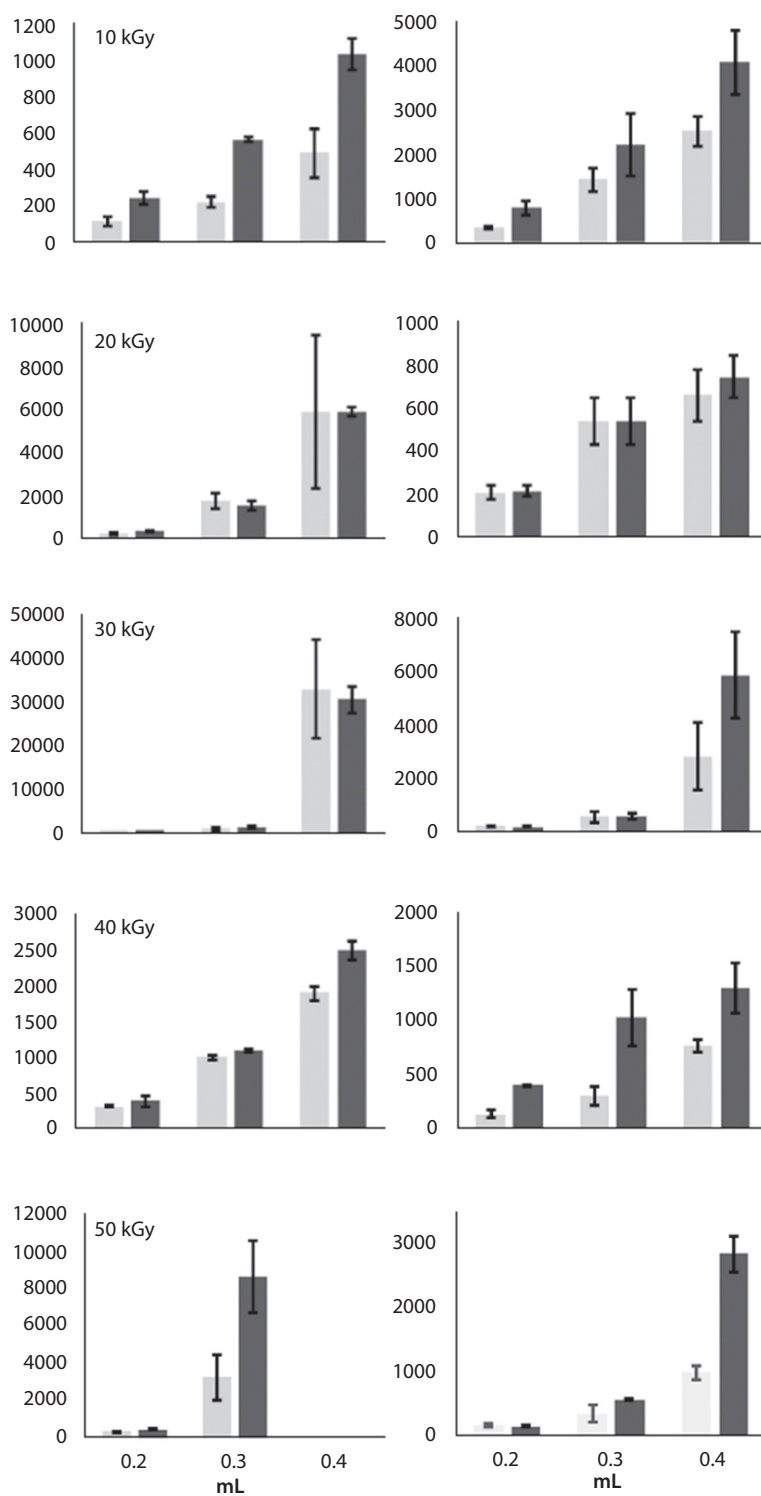
Figure 14 Comparative of sensibility (%) at different injection volumes of chloroform. DAPOHELO/MWCNT (left) and DAPAELO/MWCNT (right). Light grey (no irradiated samples), dark grey (irradiated samples at different doses). Mean values ± SD (n = 4).

of diacetylene polymer network and MWCNT at different loads. The percolation curves were plotted and the critical concentrations for diacetylene linseed oil of around 5% were lower than ELO/MWCNT composite [47], demonstrating that rich electron groups had a positive effect on the dispersion of MWNT without any modification. The calculated percolation threshold was low enough to prepare composites which were used in the sensing of chloroform, acetone and ethanol. The composites of DAPAELO and DAPOHELO had a high sensibility toward these solvents; however, the DAEAELO had a very low sensibility, showing that the effect of introducing an aromatic ring into the structure produces other interactions which avoid the chain separation in the sensing. Besides, irradiation in the chosen samples at doses higher than 20 kGy results in a diminishing thickness likely due to the crosslinking of the chains in the polymer. Irradiation resulted in changes in the sensibility and improved the reproducibility because the structure may return to its original conformation. In this work only a first approximation was done on the effect of radiation on the composite and organic vapor sensing; however, an opportunity is open to evaluate the effect of the radiation dose on the thickness and crosslinking, and these on the sensing parameters.

ACKNOWLEDGMENTS

REFERENCES

1. A. Gandini and T.M. Lacerda, From monomers to polymers from renewable resources: Recent advances. *Prog. Polym. Sci.* **48**, 1–39 (2015).
2. U. Bierman, U. Bornscheuer, M.A.R. Meier, J.O. Metzger, and H.J. Schäfer, Oils and fats as renewable raw materials in chemistry. *Angew. Chem. Int. Edit.* **50**, 3854–3871 (2011).
3. M.Y. Abduh, M. Iqbal, F. Picchioni, R. Manurung, and H.J. Heeres, Synthesis and properties of cross-linked polymers from epoxidized rubber seed oil and triethylenetetramine. *J. Appl. Polym. Sci.* **132**, 42591 (2015).
4. M.A. Mosiewicki and M.I. Aranguren, A short review on novel biocomposites based on plant oil precursors. *Eur. Polym. J.* **49**, 1243–1256 (2013).
5. G. Lligadas, J.C. Ronda, M. Galià, and V. Cádiz, Renewable polymeric materials from vegetable oils: A perspective. *Mater. Today*, **16**(9), 337–343 (2013).
6. A. Gandini, Epoxy polymers based on renewable resources, in *Epoxy Polymers: New Materials and Innovation*, J.P. Pascault and R.J.J. Williams (Eds.), pp. 55–78, Wiley-VCH Verlag GmbH & Co. KGaA, New Jersey (2010).
7. Y. Xia, R.L. Quirino, and R.C. Larock, Bio-based thermosetting polymers from vegetable oils. *J. Renew. Mater.* **1**(1), 3–27 (2013).
8. A. Köckritz and A. Martin, Oxidation of unsaturated fatty acid derivatives and vegetable oils. *Eur. J. Lipid. Sci. Tech.* **110**, 812–824 (2008).
9. H. Esen and G. Çayli, Epoxidation and polymerization of acrylated castor oil. *Eur. J. Lipid Sci. Technol.* **118**, 959 (2016).
10. T. Tsujimoto, T. Takayama, and H. Uyama, Biodegradable shape memory polymeric material from epoxidized soybean oil and polycaprolactone. *Polymers* **7**, 2165–2174 (2015).
11. R. Wang and T.P. Shuman, Vegetable oil-derived epoxy monomers and polymer blends: A comparative study with review. *Express Polym Lett.* **7**(3), 272–292 (2013).
12. R. Auvergne, S. Caillol, G. David, B. Boutevin, and J.P. Pascault, Biobased thermosetting epoxy: present and future. *Chem. Rev.* **114**, 1082–1115 (2014).
13. L. Montero de Espinoza and M.A.R. Meier, Plant oils: The perfect renewable resource for polymer science?!. *Eur. Polym. J.* **47**, 837–852 (2011).
14. R. Andrews and M.C. Weisenberger, Carbon nanotube polymer composites. *Curr. Opin. Solid St. M.* **8**, 31–37 (2004).
15. P.G. Collins, A. Zettl, H. Bando, A. Thess, and R.E Smalley, Nanotube nanodevice. *Science* **278**, 100–102 (1997).
16. E.T. Thostenson, Z. Ren, and T.W. Chow, Advances in the science and technology of carbon nanotubes and their composites: A review. *Compos. Sci. Technol.* **61**, 1899–1912 (2001).
17. R.H. Baughman, A.A. Zakhidov, and W.A. de Heer, Carbon nanotubes the route toward applications. *Science* **297**, 787–792 (2002).
18. T. Sekitani, H. Nakajima, H. Maeda, T. Fukushima, T. Aida, K. Hata, and T. Someya, Stretchable active-matrix organic light-emitting diode display using printable elastic conductors. *Nat. Mater.* **8**, 494–499 (2009).
19. L. Hu, M. Pasta, F.L. Mantia, L. Cui, S. Jeong, H.D. Deshazer, J.W. Choi, S.M. Han, and Y. Cui, Stretchable, porous, and conductive energy textiles. *Nano Letters*, **10**, 708–714 (2010).
20. H. Ago, K. Petritsch, M.S.P. Shaffer, A.H. Windle, and R.H. Friend, Composite carbon nanotubes and conjugated polymers for photovoltaic devices. *Adv. Mater.* **11**(15), 1281–1285 (1999).
21. A. Mercoçi, M. Pumera, X. Llopis, B. Pérez, M. del Valle, and S. Alegret, New materials for electrochemical

sensing VI: Carbon nanotubes. *Trends Anal. Chem.* **24**(9), 826–838 (2005).

22. W. Obitayo and T. Liu, A review: Carbon nanotube-based piezoresistive strain sensors. *J. Sensors*, **2012**, ID 652438 (2012).

23. N. Sinha, J. Ma, and J.T.W Yeow, Carbon nanotube-based sensors. *J. Nanosci. Nanotechno.* **6**, 573–590 (2006).

24. A. Eitan, K. Jiang, D. Dukes, R. Andrews, L.S. Schadler, Surface modification of multiwalled carbon nanotubes: Toward the tailoring of the interface in polymer composites. *Chem. Mater.* **15**, 3198–3201 (2003).

25. N. Roy, R. Sengupta, and A.K. Bhowmick, Modification of carbon for polymer composites and nanocomposites. *Prog. Polym. Sci.* **37**, 781–819 (2012).

26. J.E Moreno Marcelino, E. Vigueras-Santiago, G. López-Téllez, S. Hernández-López, Chemical functionalization of carbon nanotubes and its effects on electrical conductivity. *J. Nano Res.* **28**, 51–61 (2014).

27. A. López-Bezanilla, F. Triozon, S. Latil, X. Blasé, S. Roche, Effect on the chemical functionalization on charge transport in carbon nanotubes at the mesoscopic scale. *Nano Lett.* **9**(3), 940–944 (2009).

28. D. Bouilly, J. Cabana, and R. Martel, Unaltered electrical conductance in single-walled carbon nanotubes functionalized with divalent adducts. *App. Phys Lett.* **101**(5), 0531161 (2012).

29. J. Yu, N. Grossiord, C.E. Koning, and J. Loos, Controlling the dispersion of multi-walled carbon nanotubes in aqueous surfactant solution. *Carbon*, **45**, 618–623 (2007).

30. K.D. Ausman, R. Piner, O. Lourie, and R.S. Ruoff, Organic solvent dispersions of single-walled carbon nanotubes: Toward solutions of pristine nanotubes. *J. Phys. Chem. B* **104**, 8911–8915 (2000).

31. S. Hernández-López, E. Vigueras-Santiago, M. Mendoza-Mora, J.R. Farias-Mancilla, and E.A. Zaragoza-Contreras, Cellulose-based polymer composite with carbon black for tetrahydrofurane sensing. *Inter. J. Polym. Sci.* **2013**, ID 381653 (2013).

32. E. Vigueras-Santiago, S. Hernández-López, C. Hernández-Escobar, A. Zaragoza-Contreras, and J.R. Farías, Thickness effect on the solvent sensing parameters of carbon black-polymer composites. *Procedia Eng.* **87**, 184–187 (2014).

33. A. Charlesby, *Atomic Radiation and Polymers: International Series of Monographs on Radiation Effects in Materials*, vol. 1, Elsevier, Oxford (1960).

34. G. López-Téllez, E. Vigueras-Santiago, and S. Hernández-López, Characterization of linseed oil epoxidized at different percentages. *Superficies y Vacío* **22**(1), 5–10 (2009).

35. A.S. Hay, Oxidative coupling of acetylenes II. *J. Org. Chem.* **27**(9), 3320–3321 (1962).

36. B. Maaten, J. Moussa, C. Desmarets, P. Gredin, P. Beaunier, T. Kanger, K. Tõnsuaadu, D. Villemin, and M. Gruselle, Cu-modified hydroxy-apatite as catalyst for Glasser-Hay C-C homo-coupling reaction of terminal alkynes. *J. Mol. Catal. A-Chem.* **393**, 112–116 (2014).

37. P. Lahtinen, E. Lankinen, M. Leskelä, and T. Repo, Insight into copper oxidation catalyst: Kinetic, catalytic active species and their deactivation. *App. Catal. A-Gen.* **295**, 177–184 (2005).

38. K.A. Aissa, J.L. Zheng, L. Estel, and S. Leveneur, Thermal stability of epoxidized and carbonated vegetable oils. *Org. Process Res. Dev.* **20**, 948–953 (2016).

39. M. Castro Martínez, S. Hernández López, and E. Vigueras-Santiago, Relationship between polymer dielectric constant and percolation threshold in conductive poly (styrene)-type polymer and carbon black composites. *J. Nanomater.* **2015**, ID 607896 (2015).

40. S.G. Tan and W.S. Chow, Biobased epoxidized vagetable oils and its greener epoxy blends: A review. *Polym.-Plastic. Technol.* **49**, 1581–1590 (2010).

41. W.W. Nawar, Thermal degradation of lipids. A review. *J. Agr. Food Chem.* **17**(1), 18–21 (1969).

42. G. López-Tellez, E. Vigueras-Santiago, S. Hernández-López, and B. Bilyeu, Synthesis and thermal cross-linking study of partially-aminated epoxidized linseed oil. *Des. Monomers Polym.* **11**, 435–445 (2008).

43. C.X. Liu and J.W Choi, Improved the dispersion of carbon nanotubes in polymers at high concentrations. *Nanomaterials* **2**, 329–347 (2012).

44. Y.Y Huang and E.M. Terentjev, Dispersion of carbon nanotubes: Mixing, sonication, stabilization, and composite properties. *Polymers* **4**, 275–295 (2012).

45. V. Antonucci, G. Faiella, M. Giordano, L. Nicolais, and G. Pepe, Electrical properties of single walled carbon nanotubes reinforced polystyrene composites. *Macromol. Symp.* **247**, 172–181 (2007).

46. R. Rizvi and H.E. Naguib, Carbon nanotube network evolution during deformation of PVDF-MWNT nanocomposites, in *SPIE Smart Structures and Materials+ Nondestructive Evaluation and Health Monitoring. International Society for Optics and Photonics*, pp. 86871V–86871V, International Society of Optics and Photonics (2013).

47. A. Ramírez-Jiménez, S. Hernández-López, and E. Vigueras-Santiago, Conductive polymeric composites based on multiwalled carbon nanotubes and linseed oil functionalized and cross-linked with diacetylenes from propargyl alcohol. *J. Nanomater.* **2015**, ID 531249 (2015).